Deep-Sea Research, Vol. 35, No. 12, pp. 1971–1990, 1988.
Printed in Great Britain.

0198-0149/88 $3.00 +0.00

Temporal variations in the separation of Brazil and Malvinas Currents

DONALD B. OLSON,* GUILLERMO P. PODESTÁ,† ROBERT H. EVANS* and OTIS B. BROWN*

(*Received* 15 *January* 1988; *revised form* 11 *July* 1988; *accepted* 18 *July* 1988)

Abstract—The separation of the Brazil and Malvinas (Falkland) Currents from the western boundary is explored with the use of satellite and drifter data. The location of the separation of these boundary currents from the continental margin over a multiyear period is determined by digitizing the crossing of the surface thermal front indicative of each feature with the 1000 m isobath. Three years (July 1984 to June 1987) of 1 km resolution AVHRR data collected by the Argentina Meteorological Service and 4 years of lower resolution Global Retrieval Tape (GRT) data were used to generate a total time series extending from November 1981 to June 1987; i.e. 5½ years.

The mean latitudes of separation from the shelf break are 35.8 ± 1.1° for the Brazil Current and 38.6 ± 0.9° for the Malvinas Current. The along-coast ranges of the separation positions, 930 and 850 km, respectively, are quite large relative to similar statistics for the Gulf Stream or Kuroshio. Observed temporal variability suggests cyclical excursions of the currents along the coast at semi-annual and annual periods, although there is considerable interannual variation in the signal. Drifter trajectories overlaid on satellite images demonstrate events associated with the annual transition in 1984–1985. Shorter time-scale perturbations in the currents' separation latitudes occur in the 30–60 day band, which corresponds to the mesoscale eddy field. The connection of the variation in the separation with various possible forcing mechanisms is briefly discussed, along with the problem of gaining a theoretical understanding of this dynamic situation. Finally, the extensions of the two currents into the South Atlantic interior are described statistically using the high resolution data set.

INTRODUCTION

IN THE last 40 years there has been a basic understanding of the western boundary layer's fundamental role in closing the circulation of the world's subtropical gyres with publications of classic papers on frictional (STOMMEL, 1948; MUNK, 1950) and inertial theories (CHARNEY, 1955; MORGAN, 1956) for these currents. These early models, however, do not realistically consider the nature of the current's final separation from the western boundary and its re-entry into the ocean interior. Early models either computed a gyre in a closed basin (STOMMEL, 1948; FOFONOFF, 1954), imposed an essential solid zonal boundary between gyres as a boundary condition (MUNK, 1950), or only completed a local analysis of the boundary current along the coast (CHARNEY, 1955; MORGAN, 1956). The latter authors provided a brief analysis which shows a purely inertial model in two layers will separate in the sense that the upper layer may surface and cause their analysis to break down. Various other attempts to treat the Gulf Stream as an inertial boundary

* Division of Meteorology and Physical Oceanography, Rosenstiel School of Marine and Atmospheric Science, University of Miami, 4600 Rickenbacker Cswy, Miami, FL 33149, U.S.A.

† Division of Biology and Living Resources, Rosenstiel School of Marine and Atmospheric Science, University of Miami, 4600 Rickenbacker Cswy, Miami, FL 33149, U.S.A. Present address: NASA Goddard Space Flight Center, Code 671, Greenbelt, MD 20771, U.S.A.

current provided further insight into the problem in terms of necessary interior matching conditions which allow the existence of an intense boundary current (GREENSPAN, 1962, 1963; CARRIER and ROBINSON, 1962; ROBINSON, 1965; SPEIGEL and ROBINSON, 1968). These models, however, supply little or no information on the dynamics at the point of separation. PARSONS (1969) in a two-year model gave the first detailed analysis of the separation as the location at which the interface between layers' surfaces. KAMENKOVICH and REZNIK (1972) extended the analysis to allow motion in both layers. This latter work and expansion of Parsons' problem by MOORE and NIILER (1974) explored the nature of the physical balances near the separation point in terms of a rather epic presentation of perturbation methods. At about the same time, VERONIS (1973) completed a detailed analysis of the global circulation and boundary current circulation in all western boundary currents using a transport analysis whose basis is the same as that in PARSONS (1969). Recent years have not seen as much analytical activity in relation to boundary current separation, although a topographic, viscous theory by SMITH and FANDRY (1976) and a recent analysis of Agulhas by OU and DE RUIJTER (1986) have appeared.

The lack of new progress in the theoretical realm has been accompanied by observational neglect which, in part, seems to be associated with the Gulf Stream's pre-eminent place in boundary current literature. The Gulf Stream separates from the coast at Cape Hatteras in a process that has strong topographic controls (GREENSPAN, 1963; WARREN, 1963). In the present case the nature of the separation of a very different boundary current, the Brazil Current, is explored on an observational basis. While this current adds the complication of strong temporal variability, it is hoped that the results will stimulate new consideration of this important large-scale circulation question.

The Brazil Current (Fig. 1), the western boundary current associated with the subtropical gyre in the South Atlantic Ocean, flows south along the continental margin of South America to a point off Argentina and Uruguay where, in the mean, it separates from the coast at 36°S. The separation is north of the wind stress curl zero in the basin which occurs near 47° to 48°S (HELLERMAN and ROSENSTEIN, 1983). Therefore, the separation is premature as compared to the simplest idea for boundary current separation, i.e. that the separation occurs at the wind stress maximum, e.g. in Munks' choice. The actual separation latitude is essentially that predicted by VERONIS (1973) in his analysis of the global circulation with a two-layer model, even though his model is unrealistic in terms of boundary current transport. Veronis also pointed out the possible importance of the equatorward-flowing Malvinas Current in the dynamics of the Brazil–Malvinas Confluence.

The Malvinas (Falkland) Current originates as a branch of the Subantarctic Front which is the northernmost front associated with the Antarctic Circumpolar Current in the Drake Passage. The subantarctic waters bifurcate as they pass the Falkland Escarpment to the east of Maurice Ewing Bank (≈40°W); a portion of the flow moves westward along the Malvinas (Falkland) Plateau towards the Argentine shelf break, where it turns northwards. This cold, fresh subantarctic water meets the warm, saline Brazil Current, and both turn out to sea in a region known as the Brazil–Malvinas Confluence (Fig. 1).

Early descriptions of the Brazil and Malvinas Confluence include those by DEACON (1937) and DEFANT (1941). More recently, several cruises have collected oceanographic data in this area (RYZHKOV, 1966; BROSIN and NEHRING, 1967; REID *et al.*, 1977; SCHEMAINDA, 1980; GORDON, 1981; SZPIGANOWICZ, 1983; GORDON and GREENGROVE, 1986; RODEN, 1986). In addition to these hydrographic descriptions, planktonic Forami-

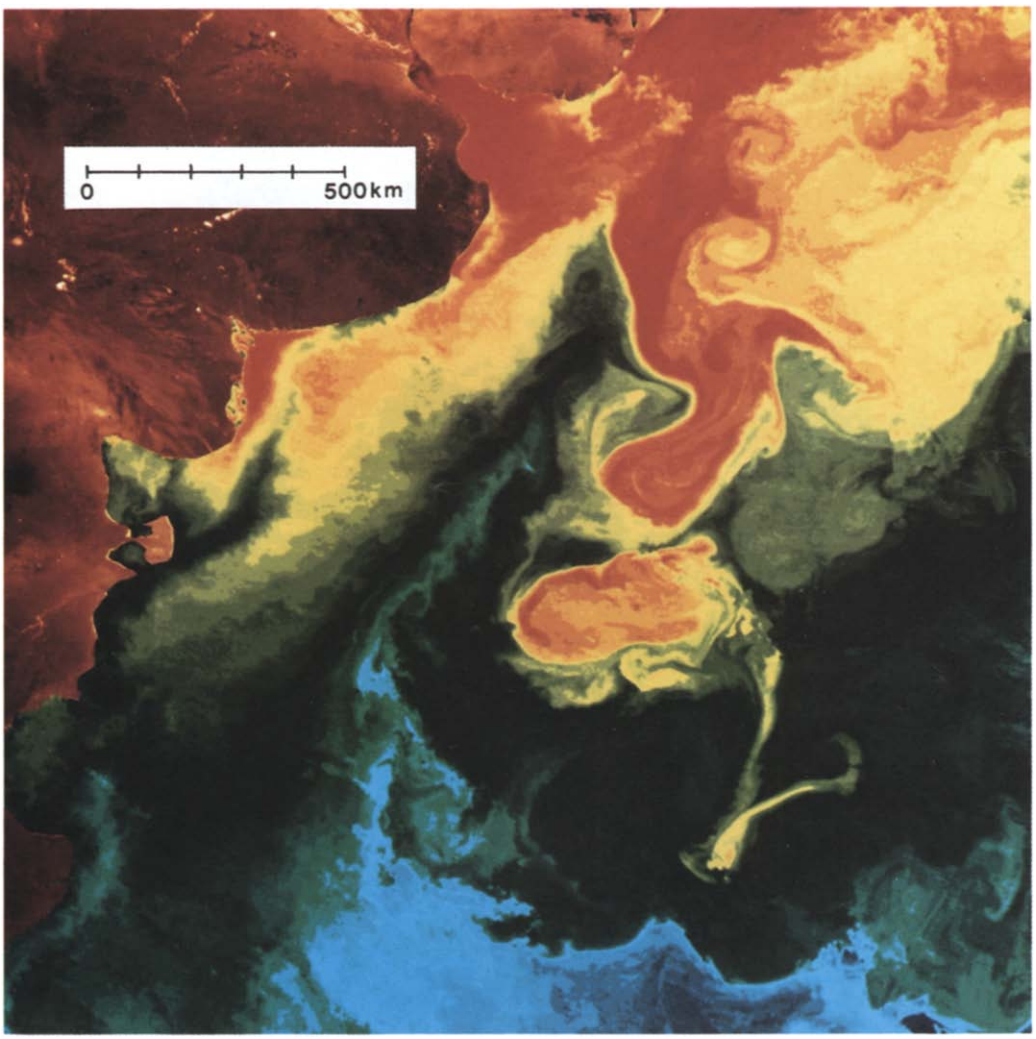

Fig. 1. Image of the Brazil–Malvinas Confluence in February 1985. Warm waters are coded in red, temperature decreases grading through yellow and green with blues being the coldest. This time frame corresponds to a southward extension of the Brazil Current and the formation of a large anticyclonic (warm) eddy or ring. Event is described in more detail in the text.

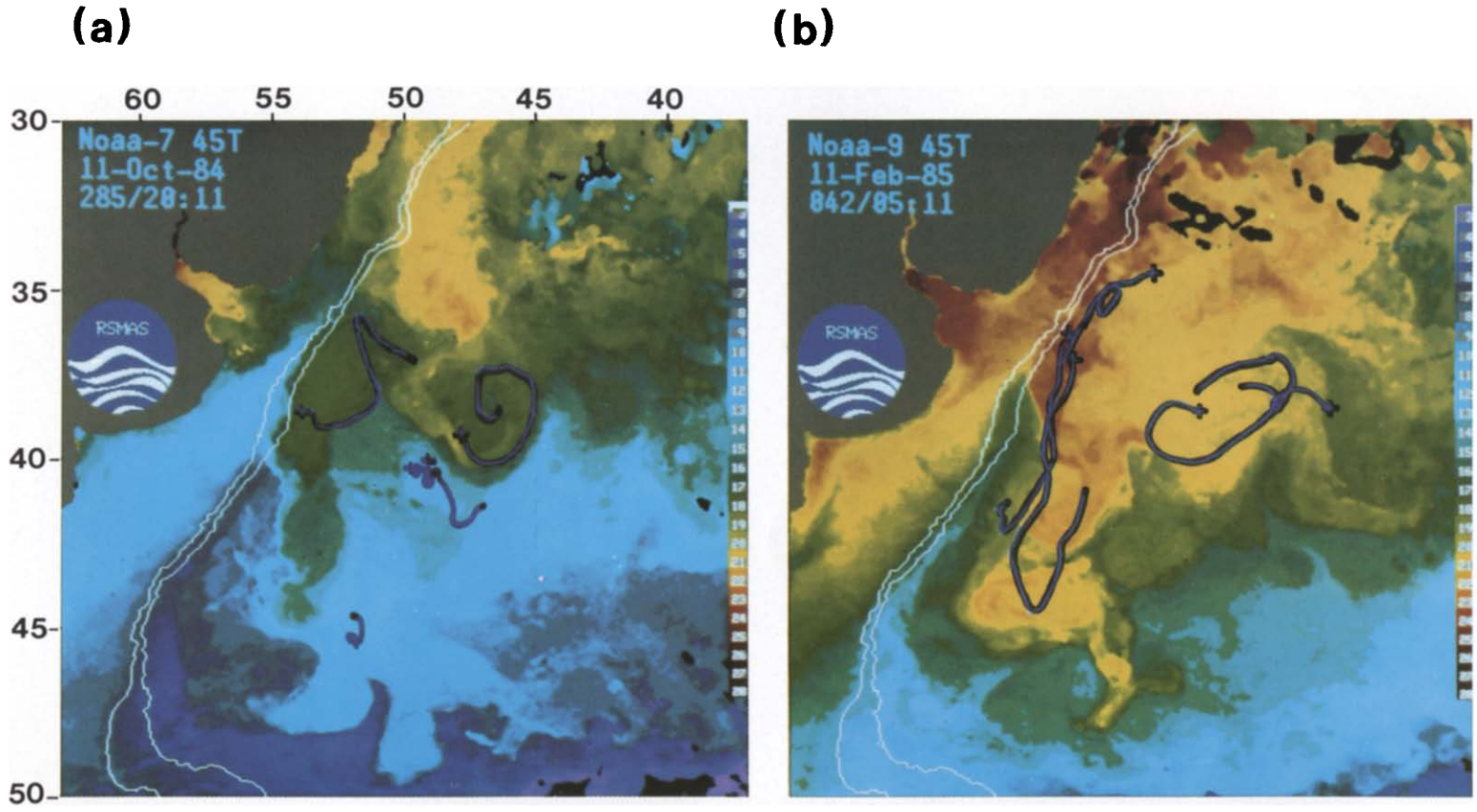

Fig. 4. Atmospherically corrected NOAA AVHRR images of the Brazil Confluence region for (a) 11 October 1984 and (b) 11 February 1985. Images are coded such that warm temperatures are dark red while cold temperatures are light blue. A temperature scale is provided along the side of each image. Drifter trajectories centered about ±20 days of (a) and ±10 days of (b) are shown in blue. The white contours are the 200 and 1000 m isobaths.

nifera have been used as biological tracers to identify the location of water masses (BOLTOVSKOY, 1966, 1970). *In situ* observations locate the confluence between 36° and 39°S in the mean (REID *et al.*, 1977). After its confluence with the Malvinas Current, the Brazil Current separates from the shelf break and enters the South Atlantic interior in a series of large amplitude meanders. A poleward extension of warm water, composed of warm eddies, filaments and meanders, is almost always present within the longitudes of 50° to 55°W and can be considered a quasi-stationary structure (GORDON, 1981). The southern limit of the warm water associated with the Brazil Current fluctuates between 38° and 46°S, with fluctuations accompanied by the intermittent formation of warm-core anticyclonic eddies (LEGECKIS and GORDON, 1982).

The Brazil Current reverses its direction between 40° and 46°S (REID *et al.*, 1977), where the poleward flow turns counterclockwise, and then proceeds northward just offshore of the poleward stream (LEGECKIS and GORDON, 1982). A full description of the path of the current and its variability is given below.

The complexity of the circulation in the confluence region became apparent after the advent of environmental satellite observations. The confluence is particularly suited for study by remote sensing techniques for two reasons: satellite-based sensors provide synoptic monitoring required to adequately describe the complex mesoscale variability of this region and the processes of interest have strong thermal signals at the ocean surface. Hydrographic surveys (cf. DEACON, 1937) find strong horizontal surface thermal gradients in the Confluence, often reaching 1°C km^{-1}; BROSIN and NEHRING (1967) reported a change of 7.5°C over a range of 3.5 nmi; LUSQUIÑOS and VALDEZ (1971) cite SST changes approaching 7°C in 15–30 nmi. Similar thermal gradients have been detected by satellite sensors: WARNECKE *et al.* (1971), using data from a radiometer onboard the NIMBUS II satellite, observed strong surface thermal gradients at the confluence of the Brazil and Malvinas Currents. TSENG (1974) and TSENG *et al.* (1977) were the first to systematically use satellite infra-red data (NIMBUS-V THIR) in this region to determine the mean position of the Brazil Current front; although their results showed motion with seasonal time scales, they did not resolve strong meridional changes in the separation latitude. LEGECKIS (1978), using NOAA VHRR imagery, found that eddy generation in this region is highly variable in time. Subsequently, LEGECKIS and GORDON (1982) observed eddy shedding in the Confluence and poleward pulsing of the Brazil Current between 38° and 46°S with a time scale of approximately 2 months.

We present here a systematic study of the Brazil and Malvinas Confluence region using satellite infra-red observations to obtain a space/time description of the currents and their attendent eddy systems. Previous studies of the convergence based on remotely sensed data have relied on a relatively small number of images. The persistent cloud coverage, however, requires a much larger data series in order to adequately comprehend the variability of the region. This work is based on a 3-year time series of NOAA Advanced Very High Resolution Radiometer (AVHRR) High Resolution Picture Transmission (HRPT) digital data acquired through Argentina's Servicio Meteorologico Nacional (National Meteorological Service) receiving facility in Buenos Aires, on 5 years of Global Retrieval Tapes (GRTs), and on a set of satellite drifting buoys launched in the confluence region in late 1984.

DATA AND METHODS

Sea surface temperature fields are derived from the AVHRR onboard satellites of the NOAA series located in sun-synchronous polar orbits with ascending passes at either

0730 or 1400 local sun time. The spectral bands of the AVHRR are described in SCHWALB (1978).

We analyse two types of satellite retrievals. Processing for the two types of satellite data is described separately. High resolution HRPT data, with a spatial resolution of approximately 1 km, were collected between July 1984 and March 1987. Over the 33 month collection period 696 passes over the convergence region were archived.

The SST estimates on NOAA/NESDIS (the U.S. National Oceanic and Atmospheric Administration/National Environmental Satellite and Data Information Service) GRT tapes are computed from Global Area Coverage (GAC) AVHRR retrievals (SCHWALB, 1978), with an effective resolution of 5 km. The AVHRR observations clustering about members of a set of first guess retrieval locations (density varies from 14 to 50 km dependent on location) are passed through a sequence of tests (MCCLAIN *et al.*, 1985) to reduce atmospheric contamination. Then, a multi-channel (MCSST) algorithm, similar to the one used for HRPT data, is applied to produce an SST estimate for each location. These data, covering the period from November 1981 until June 1987, are archived weekly.

Surface drifters tracked by the ARGOS system were launched during cruises on the R.V. *Thomas Washington* in late 1984. The units are PRL Mini-TOD units manufactured by Polar Reseach Labs, with surface mixed-layer drogues designed to float horizontally to the side of the unit. Although no specific tests have been completed on these particular instruments, tests on similar designs suggest they track the surface fluid motions to better than 5–10 cm s^{-1}. Most of the error is thought to be wave induced (NIILER *et al.*, 1987).

HRPT data processing

Satellite infra-red SST determination is affected by several environmental factors which degrade the accuracy of the satellite-derived temperature. The major sources of error in the radiometric determination for AVHRR channels 4 and 5 include water vapor absorption in the lower atmosphere and aerosol absorption. Water vapor correction algorithms are based on the observation that the integrated atmospheric transmittance differs among the AVHRR infra-red channels; consequently, the temperatures sensed at each channel will also differ (ANDING and KAUTH, 1970; PRABHAKARA *et al.*, 1974). The SST is computed using a multi-channel algorithm for AVHRR channels 4 and 5 (MCCLAIN *et al.*, 1983).

All SST imagery is mapped to a fixed geographic grid using a cylindrical equi-rectangular projection covering the area from approximately 30° to 50°S and 63° to 37°W (pixels along the 40°S latitude are equal area). Cloudiness in this area of the South Atlantic is a major problem for infra-red SST determination, particularly during winter months. Each image is cloud filtered and composited into a 5-day mosaic using a warmest pixel approach. In this fashion, 122 5-day composites are obtained from the original 696 individual passes; these composites form the basis for subsequent analyses.

RGSTA data processing

The SST estimates archived on the "Global Retrieval Tapes" are the basis of the RSMAS (University of Miami Rosenstiel School of Marine and Atmospheric Science) Global Surface Temperature Analysis (RGSTA). A cylindrical equi-rectangular grid with element size of (18 × 18 km) is defined: the grid has dimensions of 2048 (longi-

tude) × 1024 (latitude). SST estimates are binned at bi-weekly intervals using day-time retrievals since there is evidence that nightly retrievals are contaminated by sensor thermal cycling (BROWN *et al.*, 1986). Due to the effects of cloudiness or other environmental factors, the resultant fields are not completely filled. A Laplacian relaxation technique is used to interpolate values in data voids. An iterative procedure is employed to fill void grid locations: extant SST estimates that encompass data voids are fixed and used as boundary conditions; the previous bi-weekly first guess field is used as an initial estimate; SST estimates in these areas are then relaxed until Laplace's equation is satisfied. A region is coded as cloudy if the data void area exceeds 130 km; interpolation effects are reduced to smaller scales.

SEPARATION FROM THE COAST

The Brazil Current, as distinguished by a continuous band of warm subtropical surface water extending southward along the coast, separates from the continental shelf and slope in the mean at 35.8°S, with a standard deviation of 1.1° (213 km for the along-coast

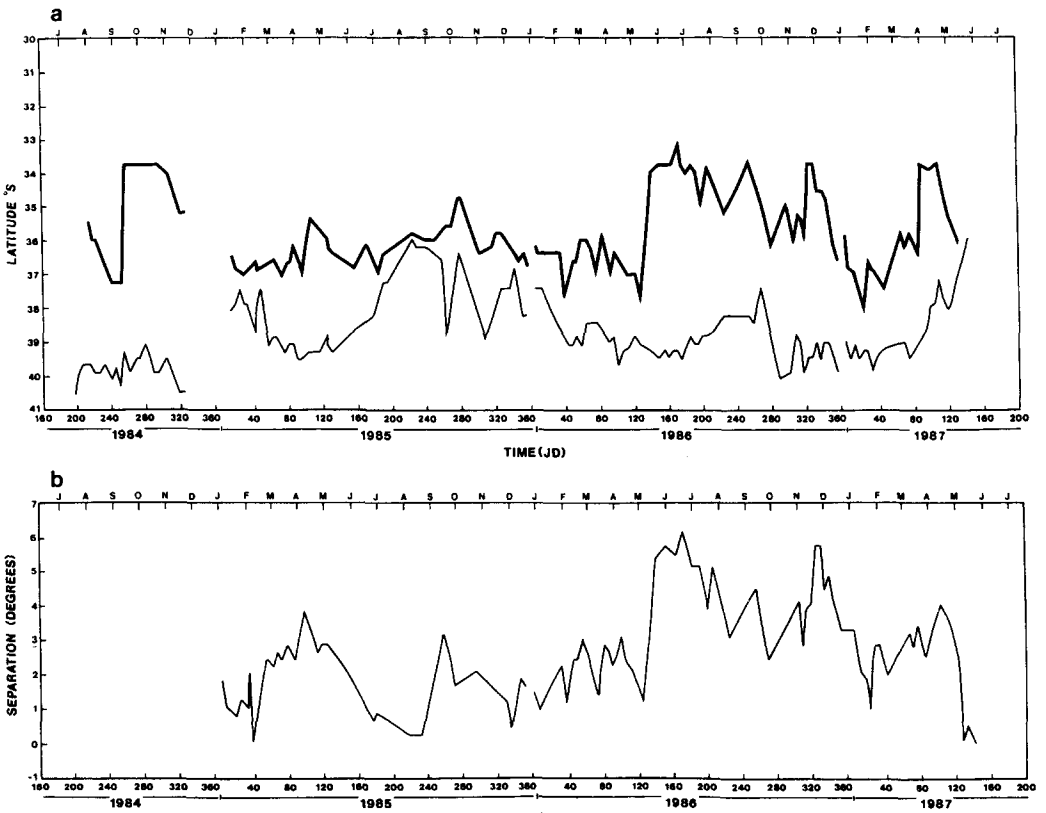

Fig. 2. Time series of separation latitudes derived from NOAA AVHRR HRPT observations. (a) Brazil Current (heavy line) and Malvinas (thin line) separation from the 1000 m isobath. (b) The distance between the two separation locations in time. Separations are given in degrees of latitude.

distance assuming a constant orientation of 35°T). This is determined by digitizing the location where the continuous western front of the warm water leaves the coast and crosses the 1000 m isobath. Digitizations using the 200 m isobath on the imagery produce similar but noisier results. The time history of the separation point is shown in Fig. 2a. The total range in latitude of the separation is 4.8° (920 km). The distribution (Fig. 3a) is somewhat skewed to the north with a weak but significant bimodal character. The major peak in a histogram (Fig. 3a) of the separation latitude occurs near 36°S (46% of the observed positions are in the bin 36° to 37°S), with a secondary peak between 33.2° and 34.0°S. The northern mode in the distribution is associated with a topographic feature extending outward from the continental shelf. Brazil Current separation is farther north in southern winter (July to September) than it is in the summer (January to March). The significance of these data is established and quantified below in relation to surface drifter data and the signal's nature relative to expected seasonal problems with the interpretation of the SST signal.

Alternatively, the northernmost extension of the cold Malvinas waters along the coast on the southern side of the confluence can be tracked (Fig. 2a). Again, a seasonal trend is apparent with a tendency for more northerly separations in the winter months. The Malvinas Current separates from the coast at a mean latitude of 38.8°S, with a standard deviation of 0.9° (170 km) and a range of 4.4° (850 km). Unlike the Brazil Current, the Malvinas separation is unimodal about the mean separation point (Fig. 3a). The Malvinas Current separation is not usually spatially coincident with the separation of the Brazil Current, but there typically is a band of intermediate temperature surface waters, up to 300 km wide, separating the two strong thermal fronts associated with the two boundary currents. The width of this zone between the two fronts as a function of time is shown in Fig. 2b. This transition zone between the subtropical boundary current extension and the subantarctic front, i.e. the Malvinas, is filled with eddies. It can be traced as a coherent separation between the fronts far into the ocean interior as shown below and in RODEN (1986).

The connection of the sea surface thermal field to the flow can be tested based on satellite drifting buoy trajectories and inverted echo sounder (IES) records near the mean Brazil Current separation location (GARZOLI and GARRAFFO, 1989). Satellite images are compared with trajectory data based on the satellite drifters in Fig. 4 for two examples of extreme separation situations. The figure presents images of the area for October 1984, when the Brazil Current separation was at a northern extreme, and February 1985, when it was undergoing a southward excursion. In October 1984, the Brazil Current as indicated by the warm fluid coming down the topography from the north leaves the coast around the topographic irregularity off southern Brazil. There is a large area of intermediate temperature waters between this separation and the cold Malvinas waters far to the south. A drifter launched in the southward flow along the coast off Argentina actually traces out the edge of a large anticyclonic eddy, re-enters the coastal domain and then follows the separating Brazil Current, as determined from the SST distribution, out away from the coast over the 20-day period of the trajectory. This is in contrast to the situation in February 1985 (Fig. 4b) when three drifters initially to the north moved rapidly (O : 1 m s^{-1}) to the south following the front from its separation from the coast into a large anticyclonic meander offshore. In the case of Fig. 4b only 10 days of trajectory are shown to simplify the presentation in this case with the rapid flows. The drifters continue around the meander to the south and enter the Brazil Extension

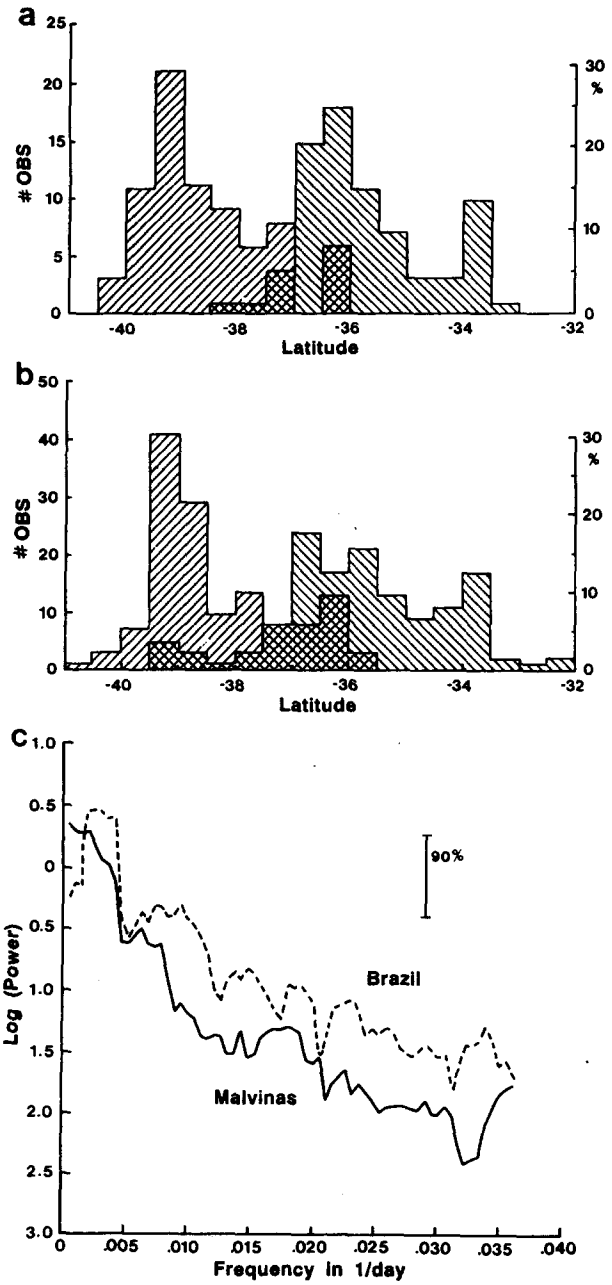

Fig. 3. Histograms of the separation latitude for the high resolution time series (a) and the RGSTA observations (b). Histograms to the left in both are for the Malvinas (upper right to lower left hatching). Cross-hatched areas denote overlapping of the Malvinas and Brazil Current histograms. (c) Spectra of the Brazil and Malvinas Currents' separations from the 1000 m isobath based on the RGSTA data set.

after the portion of trajectory shown in Fig. 4b. In conclusion, the drifter motion supports the SST analysis with relation to the flows, at least in this one realization of two extreme conditions and the transition between them.

The comparison of the satellite-derived separation histories with the echo sounder dynamic heights is very good, with discrepancies in the order of 50 km or less for IES estimated frontal position vs that determined from the imagery. The largest errors occurring in the intercomparison involve interpretation problems in the limited area IES array where an eddy such as that shown in Fig. 4a is assumed to be the Brazil Current itself. In general the longer period signal seen in the IES derived dynamic height time series (11/84 to 3/86, GARZOLI and GARRAFFO, 1989) are in complete agreement with the motion of the current separations shown in Fig. 2. A full intercomparison of the IES and surface satellite thermal pattern will be described in a subsequent paper.

The RGSTA data set from November 1981 to early January 1987 is analysed in the same manner as the higher resolution data discussed above to provide a longer time series (Figs 3b and 5). Again, the separation has distinctive events when the Brazil Current extends to the south in December to February. While the separation of the Brazil Current extends to the south near the turn of the year, it is not correct to say there is an annual or seasonal cycle, since there is not sufficient evidence for any harmonic in a statistical sense. The results of a spectral analysis of the time series are described below after an intercomparison of separation statistics from the RGSTA and HRPT data sets. These statistics can be compared to those derived from the higher resolution HRPT data after interpolation of the two series to a common temporal sampling scale corresponding to the 2-week RGSTA sampling. This is accomplished using a spline.

The latitudes of separation of the Brazil and Malvinas Currents derived from both data sets are significantly correlated at the 99% level, although the cross correlations are fairly low O : ~0.50. The Brazil Current separation has a –0.03° bias between the HRPT and RGSTA data and a standard deviation of 1.2° while the same statistics for the Malvinas separation are +0.5° and 0.9°, respectively. Differences in the statistics obtained from the two satellite data sets are small and are possibly due to the RGSTA spatial and temporal averaging, i.e. 2 weeks and 60 km. The large standard deviation is mostly the result of major discrepancies between data sets during large meridional shifts. Rapid transitions are poorly resolved in the RGSTA data and also coincide, at least twice in the overlapping data set, with gaps in the HRPT data due to receiving station difficulties (Fig. 2).

Full statistics, including a breakdown into quartiles, are given in Table 1. Discrepancies between the two data sets in the current's separation latitudes are dominated by a few outliers associated with times of rapid change; the general separation histograms, however, agree well, as shown by the quartile distributions. This is manifested in the differences between the two sets, with the Brazil (RGSTA–HRPT) data being skewed southwards and the Malvinas set northwards. Again, in comparison with the differences in the individual histograms as summarized in Table 1, this skewness is dominated by short-term excursions missed by either the temporal or spatial sampling in the RGSTA or perhaps, alternatively, the higher eddy dominated noise in the filaments of warm and cold fluid as seen in the high resolution data set. The fact that the RGSTA data have higher variances is due to a general growth in the overall variability, with longer data records (as discussed below) in relation to spectra of the time series.

In order to consider the current separations' temporal behavior and the relation

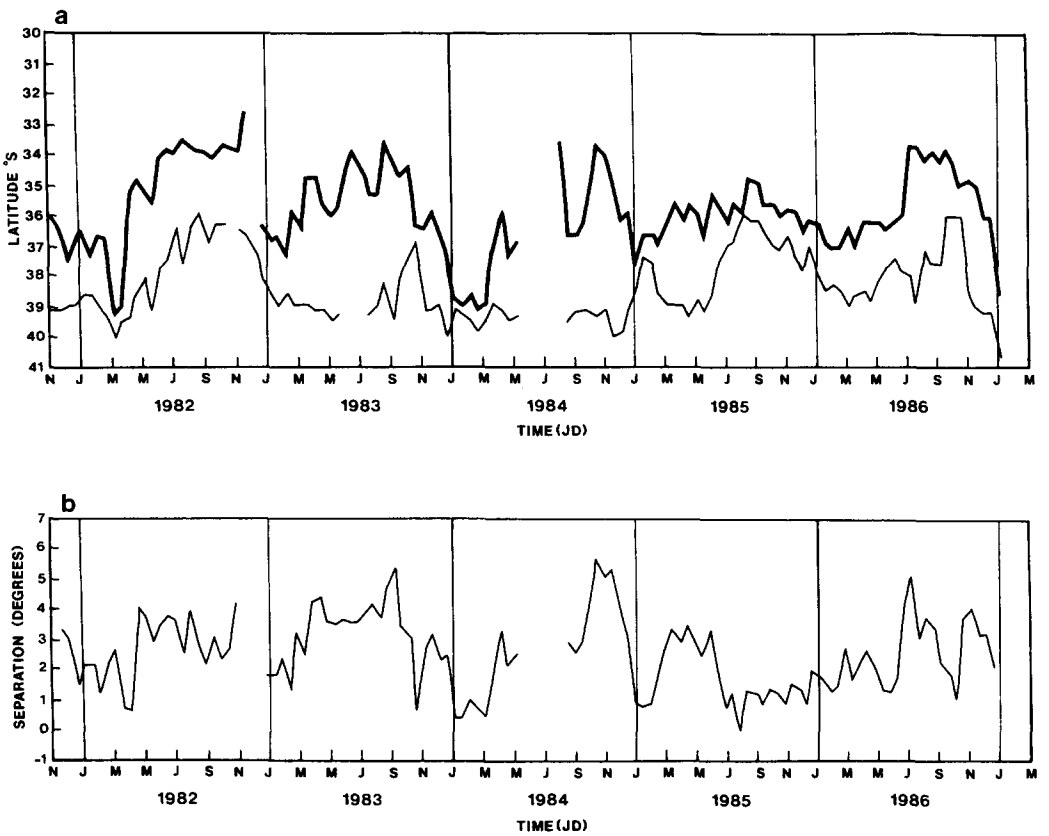

Fig. 5. Time series of separation latitudes derived from RGSTA observations. (a) Brazil Current (heavy line) and Malvinas (thin line) separation from the 1000 m isobath. (b) The distance between the two separation locations in time. Separations are given in degrees of latitude.

Table 1. *Statistics for Brazil and Malvinas separations from the coast based on* 14*-day data sets. Separation is measured relative to the* 1000 m *isobath. For details see text*

Col	*N*	Mean	S.D.	Min	25%	50%	75%	Max
Brazil Current								
HRPT data set (1984–1987)								
1	74	-35.75	1.151	-38.31	-36.56	-36.02	-35.18	-33.25
RGSTA data set (1981–1987)								
1	135	-35.70	1.475	-39.25	-36.61	-35.88	-34.62	-32.03
Malvinas Current								
HRPT data set (1984–1987)								
1	75	-38.61	1.055	-40.27	-39.34	-38.92	-37.86	-36.11
RGSTA data set (1981–1987)								
1	135	-38.36	1.134	-40.55	-39.24	-38.78	-37.51	-35.86

between them a spectral analysis is performed on the 14-day interpolated series. This analysis shows the time series produced by the two observational products with their different time periods to be different. The higher temporal coverage provided by the HRPT data has a fairly white spectrum as compared to the RGSTA data. The high resolution time series, which is also more limited by series length, shows the Brazil Current to have a peak at a period indistinguishable from the annual, while the Malvinas has a semi-annual component. Neither of these peaks is significant at the 95% level. The RGSTA data shown spectrally in Fig. 3c are more red with the Malvinas energy increasing towards lower frequencies and with only a hint of an annual peak. The Brazil Current separation in the RGSTA series has a broad peak significant at the 95% level, between 300 and 130 days period. There is coherence between the Malvinas and Brazil Current series at the 134-day period at 90% confidence. The phase between the series at this frequency is indistinguishable from zero, +5 to –43° at 95% with a best estimate of –23°, i.e. the Malvinas leads by approximately 30 days.

BRAZIL–MALVINAS EXTENSIONS

The extension of the Brazil and Malvinas Currents offshore from the confluence region is traced from the separation points determined in the previous sections using monthly mean SST images derived from the HRPT fields. The extension of the surface current pattern was assumed to follow the thermal pattern in the images. This leads to the digitization (Fig. 4a) of the warm yellow-coded, 21°C, waters for the Brazil Current and the edge of the light greenish-blue for the Malvinas. The result (Fig. 4b) follows the yellow, 21°C, water and the greenish-blue, 16°C, water for the Brazil and Malvinas, respectively. This choice is not unique and probably does not follow the exact core of the current. It is, however, a reproducible technique that corresponds to a surface water mass property definition of the current fronts. Use of thermal fields to trace boundaries between water masses may be affected by differential seasonal warming and cooling. Temperature values are extracted from HRPT imagery of the southern part of the Brazil Current and the northern part of the Malvinas Current to determine the impact of this effect. The seasonal temperature cycles for both currents show similar timing with the temperature difference between the two currents remaining fairly constant throughout the year.

Examples of the extension outlines for thermal summer (January to March) and spring (October to December) for both currents are shown in Fig. 6. These two time periods are chosen as indicative of the extremes in frontal geometry since there is a tendency for southward excursions of the Brazil Current to occur between these two periods (Figs 2 and 5).

The percentage occupation of fronts for the 33 month time series binned on a 1° grid are presented in Fig. 7. The frequency distribution of the Brazil Current extension is much more diffuse than the Malvinas. The latter has a distinctive modal position with percentage occupancies between 60 and 75%, while the mode for the Brazil Current is characterized by occupation frequencies between 45 and 60%. Both modal paths, i.e. most likely locations, execute a southward meander, followed by a northeastward trend. A summation of the percentage occupation with respect to longitudinal bands in the interior produces total occupancies for 1° ranges greater than 100%. These statistics suggest the frontal path crosses longitudinal bands twice on the average in a given

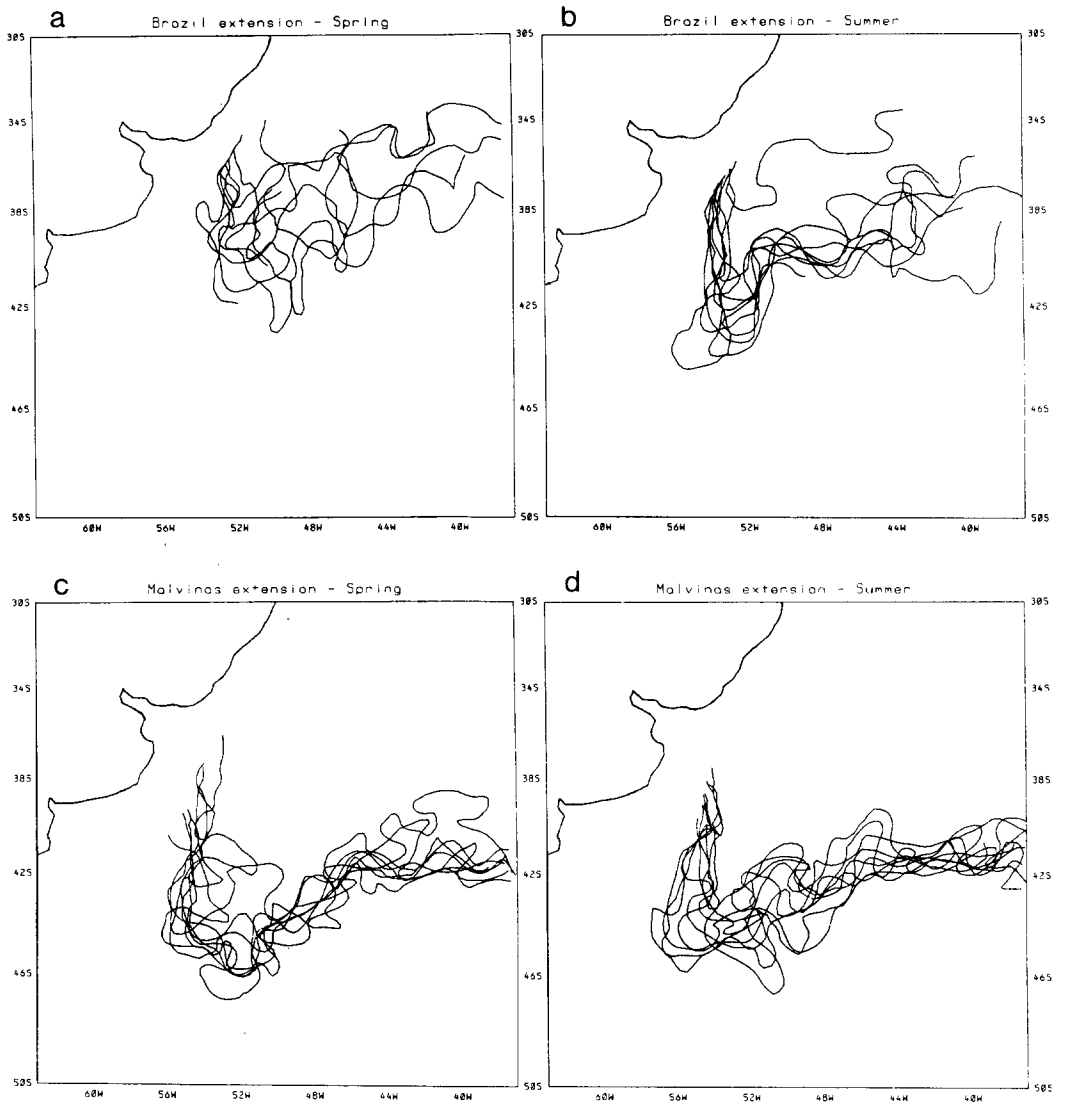

Fig. 6. Digitized traces of the Brazil Current extension in (a) southern hemisphere thermal spring and (b) summer. The same seasons for the Malvinas extension are shown in (c) and (d). Digitization follows the thermal field starting from the point in each image chosen as the separation for the current in a given month. Images are algebraic means of HRPT data after cloud removal.

realization, i.e. the monthly paths are extremely contorted by meanders where the fronts make significant north–south excursions and, in many cases, even reverse on themselves.

The two fronts are fairly close together in terms of their modal positions as they leave the coast and complete the large anticyclonic turn to the southeast. They then separate as they continue to the northeast. The region between them is filled with a vigorous eddy field made up of high amplitude meanders and detached rings and eddies. These are

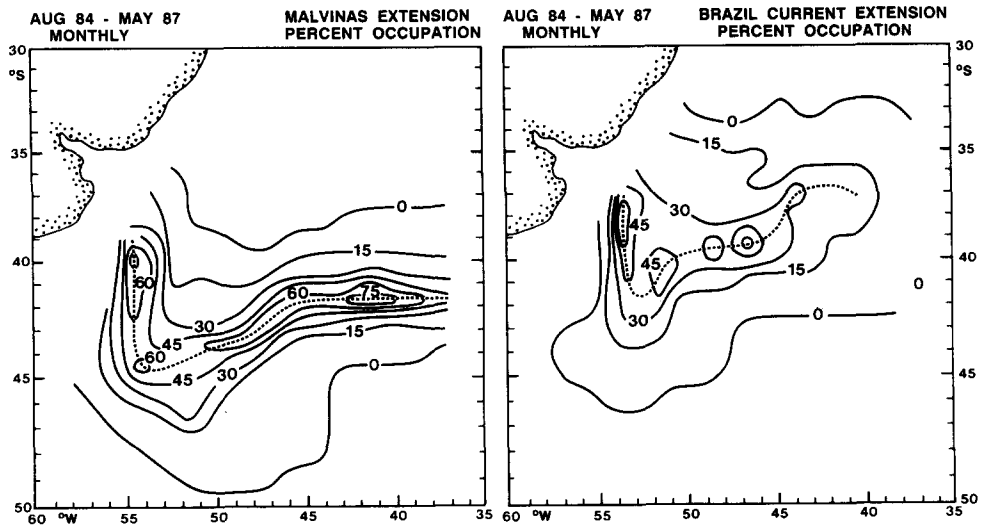

Fig. 7. Percentage occupancy for the Malvinas and Brazil Current extensions as determined from the monthly averaged HRPT data. The dashed line shows the modal position of the currents. See text for explanation of the method used for following the currents.

evident in the satellite images shown in Fig. 4. The fronts remain separated at least as far east as RODEN's (1986) survey at 41°W where they encompass an eddy filled zone 100–200 km wide.

The boundary current separations' temporal behavior and its possible influence on the boundary currents extensions are visible in Fig. 6. Differences occur primarily in the Brazil Current where both the path and the spatial variability changes between spring and summer. This is manifest by a more southward extension of the current in summer and a more variable path in spring. The other months (not shown) have intermediate patterns. Spatial variations in the Malvinas extension are less than those observed in the Brazil Current.

DISCUSSION AND CONCLUSIONS

Changes in the separation point and the downstream geometry of the current extensions in the Brazil–Malvinas system are much larger than those observed in the Gulf Stream and Kuroshio. A major portion of this difference is undoubtedly related to differences in shelf edge topography. The Argentine shelf edge is reasonably constant both in orientation and cross shelf/slope topographic profile as compared to the abrupt changes in orientation and bottom depth in the two major northern hemisphere boundary currents. The tendency for large anticyclonic features to form upon separation of the current from the shelf is completely absent in the Gulf Stream case, although it does appear to occur in the Kuroshio (TOMOSADA, 1986; KAWAMURA *et al.*, 1986).

The most comparable boundary current is probably the East Australian Current, which, like the Brazil Current, has an anomalously low transport as compared to the flow expected by integration of the wind stress over the associated subtropical gyres (VERONIS, 1973). Both have slowly varying topography, therefore reducing topographic controls

that can force boundary layer separation (GREENSPAN, 1963). The general geometry of the East Australian Current upon separation from the coast is very similar to the observations shown above (NILSSON and CRESSWELL, 1980; CRESSWELL and LEGECKIS, 1986; MULHEARN, 1987), with the current leaving the coast to form an elongated anticyclonic meander before trending back to the northeast. The temporal dependence also is similar with respect to the episodic formation of extremely large warm rings from the boundary current extension.

A major unknown in the problem of the separation variability is the nature of the responsible forcing. It is possible that wind stress variations over the South Atlantic lead to transitions in the boundary current separation. The wind stress curl from HELLERMAN and ROSENSTEIN (1983) is shown for February and June in Fig. 8a and b that represent the

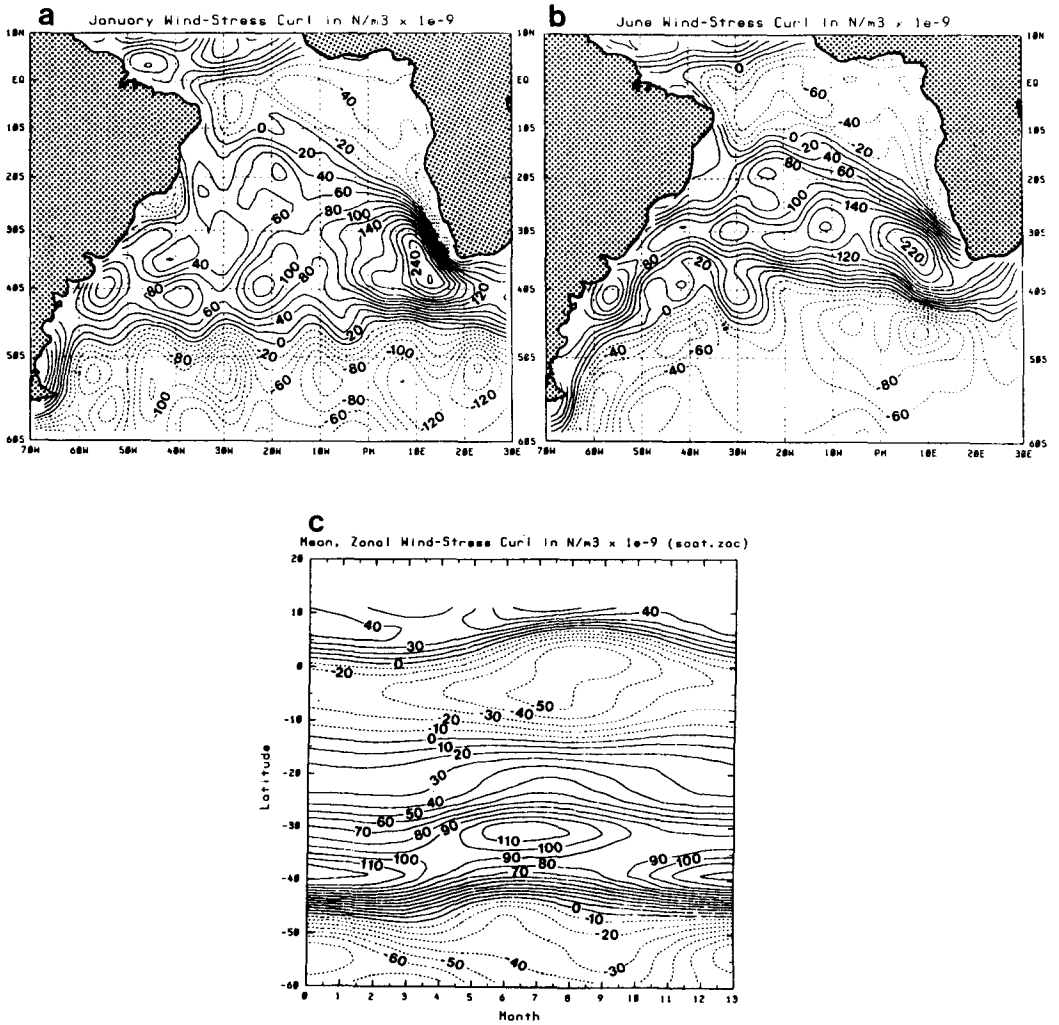

Fig. 8. Wind stress curl distributions from HELLERMAN and ROSENSTEIN (1986) data set. (a) February, (b) June. (c) Zonal mean wind stress curl plotted as a function of latitude and month. Stress curls are given in units of 10^{-9}N m^{-3}.

pattern at the two extremes in the annual cycle. The zonal average wind stress curl as a function of latitude and month is given in Fig. 8c. The low latitudes in the basin are dominated by an annual cycle in wind stress curl. South of 25°S this is superimposed on a semiannual component. Spatially these changes are manifest by major shifts in the curl distribution over the central portion of the basin (Fig. 8a, b). BRANDHORST and CASTELLO (1971) and ZYRYANOV and SEVEROV (1979) suggested that the Brazil Current separation is coincident with small-scale changes in the wind field along the South American coast. The local stress curl over the Brazil–Malvinas Confluence is fairly complicated, with the continuous anticyclonic curl over the region more localized in the winter than in the summer. It is unlikely the local stress is completely responsible for the mean location of the separation although it may play a role in the variations in separation latitude. The nature of the phase relationships between wind stress and separation variations are uncertain. Part of this uncertainty is probably inherent in the interannual variability, i.e. the use of climatological winds in comparison with a fairly short time series of separation statistics can not adequately define an interrelationship.

Finally, the relation of weak Brazil Current transport to the possible role of wind stress variations requires discussion. In the Gulf Stream or Kuroshio one does not expect major changes in transport with the shifts in seasonal winds since changes in the Sverdrup transport are small in comparison with the current transports, even if they are completely manifest in boundary current transport changes. The same is not true in the Brazil Current, where a four million cubic meter per second annual variation, such as observed in the Florida Straits, would represent a 20% change in the Brazil Current at its separation (GORDON and GREENGROVE, 1986) compared to a 4–8% change in the Gulf Stream near its separation latitude. The range of Gulf Stream percentages stems from the use of HALKIN and ROSSBY's (1985) estimate of approximately 90 Sv at 73°W for the lower and the 53 Sv estimate at Cape Fear of RICHARDSON *et al.* (1969) for the higher.

Alternatively, variations in the Brazil–Malvinas Confluence might be driven by changes in the Malvinas forced by variations in the Antarctic Circumpolar Current. Pressure changes in the Subantarctic Front where it splits to form the Malvinas can be transmitted as topographic waves (Kelvin-type response with the topography to the left in the southern hemisphere) and therefore effect the dynamics at the Confluence. Advective changes associated with transport fluctuations, similar to those envisioned due to wind changes over the subtropical gyre are also possible links between the Antarctic sector and the Confluence. Little can be said concerning these possible relationships given current data resources. The Subantarctic Front in the Drake Passage, however, is highly variable at the 1–2 month periods (WHITWORTH, 1983) although little is known about its annual and interannual variability.

There is a possibility that the separation region is influenced by the westward propagation of long meanders set up in the boundary current extension. The offshore meander field in the Brazil–Malvinas system includes very high amplitude meanders where some of the drifters remained trapped for several months. A large anticyclonic circulation evident in Fig. 4 is present for long periods of time. One drifter spent 8 months in the general area of the separation, much of this time in anticyclonic circulations (Fig. 9). In December and early January, when the satellite-derived Brazil extension is in a fairly zonal configuration, several drifters are entrained out of this anticyclonic recirculation and back westward towards the coast. At the same time other drifters launched northward in the Brazil Current accelerate and enter the separation

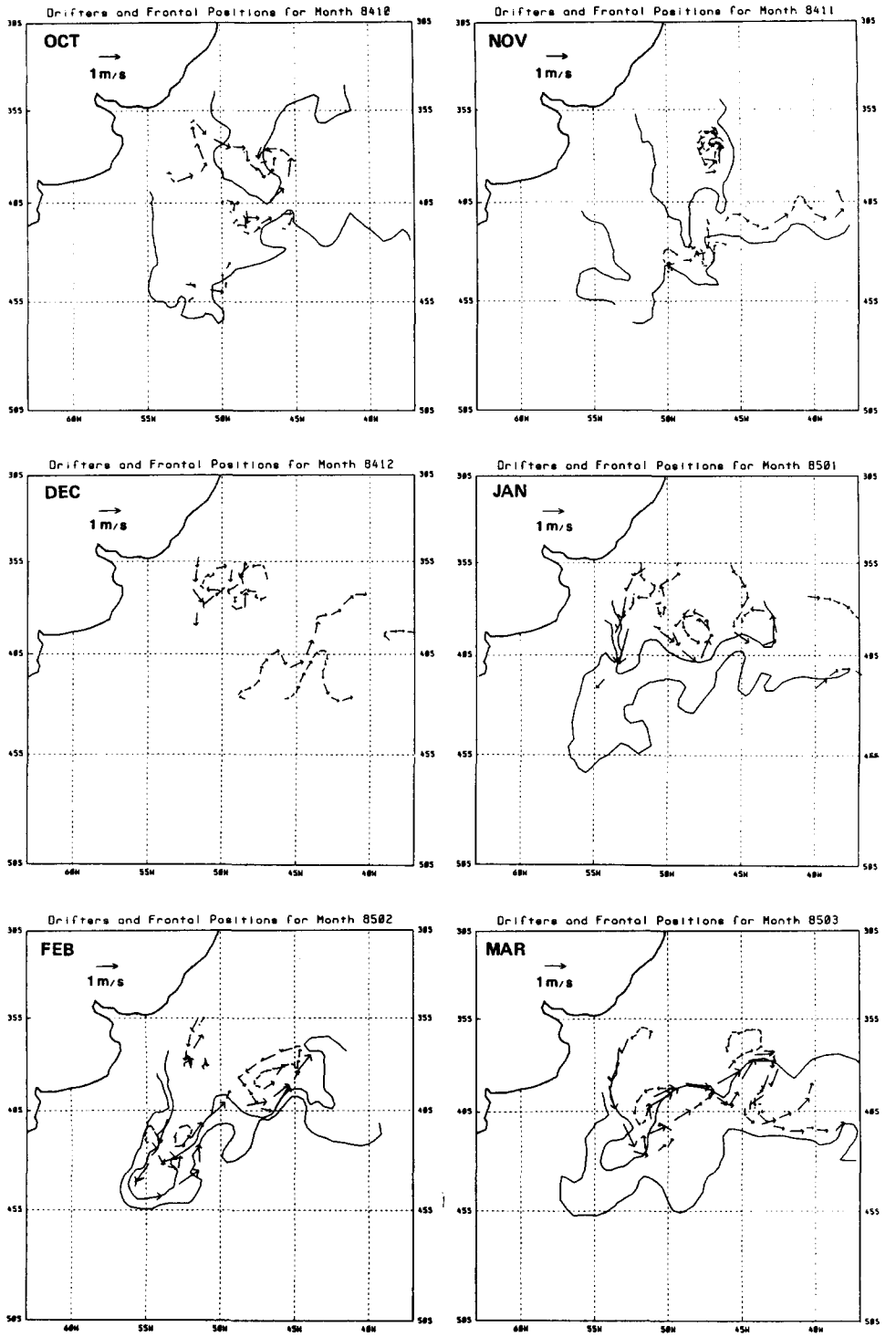

Fig. 9. Monthly summaries of frontal positions and drifter velocities for the period October 1984 to March 1985. This period corresponds to one of the major shifts in Brazil Current separation latitude as displayed in Figs 2 and 4. The fronts are digitized from the monthly averaged HRPT data. Drifter velocity vectors are for daily periods.

region (Fig. 9). Whether this is connected with propagation of the anticyclonic region into the boundary is unknown, but if this is the case, the expected result would be an increase in flow at the boundary. This is consistent with the increased velocities shown in the figure. The last panel in Fig. 9 shows drifters moving rapidly down the Brazil extension as the current returns to a more zonal configuration after the large southward pulse shown in Figs 1 and 4.

Acknowledgements—The authors would like to acknowledge the work of Ms Joanie Splain and Messrs Angel Li and Steven Emmerson in computer software, statistics generation and data processing. The high resolution AVHRR data used in this study were collected at Estación APT-AR (Villa Ortúzar, Argentina) by Servicio Meteorológico Nacional, Fuerza Aérea Argentina, as part of a cooperative study with the University of Miami. The drifter launches were accomplished on cruises made under the leadership of Arnold Gordon and Mike McCartney, whose cooperation and efforts are appreciated. Stan Hooker's help with the drogue fabrication and the logistics involved with launching the drifters is appreciated. Christina Forbes helped with some of the digitization work on the HRPT data set. Support of the Office of Naval Research under contract N00014-85-C-0020 is gratefully acknowledged.

REFERENCES

ANDING D. and R. KAUTH (1970) Estimation of sea surface temperature from space. *Remote Sensing of the Environment*, **1**, 217–220.

BOLTOVSKOY E. (1966) La zona de convergencia subtropical/subantártica en el Océano Atlántico (parte occidental). *Publceción Servicio* de *Hidrografia Naval H640*, Buenos Aires, Argentina, 69 pp.

BOLTOVSKOY E. (1970) Masas de agua (característica, distribución, movimientos) en la superficie del Atlántico sudoeste, según indicadores bioloógicos–Foraminíferos. Publceción Servicio de Hidrografia Naval H643, Buenos Aires, Argentina, 99 pp.

BRANDHORST W. and J. P. CASTELLO (1971) Evaluación de los recursos de anchoíta (*Engraulis anchoita*) frente a la Argentina y Uruguay. I. Las condiciones oceanográficas, sinópsis del conocimiento actual sobre la anchoíta y el plan para su evaluación. Proyecto de Desarrollo Pesquero. Serie Informes Técnicos **29**, 63 pp.

BROSIN H. J. and D. NEHRING (1967) Some results of oceanographical observations in the convergence area between the Falkland Current and the Brazil Current. ICES C.M. 1967/C:3.

BROWN O. B., J. W. BROWN and R. H. EVANS (1986) Calibration of advanced very high resolution radiometer infra-red observations. *Journal of Geophysical Research*, **90**, 11,667–11,678.

CARRIER G. F. and A. R. ROBINSON (1962) On the theory of the wind driven ocean circulation. *Journal of Fluid Mechanics*, **12**, 49–80.

CHARNEY J. G. (1955) The Gulf Stream as an inertial boundary layer. *Proceedings of the National Academy of Science, U.S.A.*, **41**, 731–740.

CRESSWELL G. R. and R. LEGECKIS (1986) Eddies of southeastern Australia. *Deep-Sea Research*, **33**, 1527–1562.

DEACON G. E. R. (1937) The hydrology of the southern ocean. *Discovery Reports*, **15**, 1–124.

DEFANT A. (1941) Quantitative Untersuchungen zur Statik und Dynamik des Atlantischen Ozeans. *Wissenschaftliche Ergebnisse der Deutschen Atlantischen Expedition "Meteor"*, **6**(2) (5), 191–260.

FOFONOFF N. P. (1954) Steady flow in a frictionless homogeneous ocean. *Journal of Marine Research*, **13**, 254–262.

GARZOLI S. L. and Z. GARRAFFO (1989) Transports, frontal motions and eddies at the Brazil–Malvinas Currents Confluence. *Deep-Sea Research*, submitted.

GORDON A. L. (1981) South Atlantic thermocline ventilation. *Deep-Sea Research*, **28**, 1239–1264.

GORDON A. L. and C. L. GREENGROVE (1986) Geostrophic circulation of the Brazil–Falkland Confluence. *Deep-Sea Research*, **33**, 573–585.

GREENSPAN H. P. (1962) A criterion for the existence of inertial boundary layers in oceanic circulation. *Proceedings of the National Academy of Science, U.S.A.*, **48**, 2034–2039.

GREENSPAN H. P. (1963) A note concerning topography and inertial currents. *Journal of Marine Research*, **21**, 147–154.

HALKIN D. and T. ROSSBY (1985) The structure and transport of the Gulf Stream at 73°W. *Journal of Physical Oceanography*, **15**, 1439–1452.

HELLERMAN S. and M. ROSENSTEIN (1983) Normal monthly wind stress over the world ocean with Error estimates. *Journal of Physical Oceanography*, **13**, 1093–1104.

KAMENKOVICH V. M. and G. M. REZNIK (1972) A contribution to the theory of stationary wind-driven currents in a two-layer liquid. *Izvestya, Atmospheric and Oceanic Physics*, **8**, 238–245.

KAWAMURA J., K. MIZUNO and Y. TOBA (1986) Formation process of a warm-core ring in the Kuroshio–Oyashio frontal zone—December 1986–October 1982. *Deep-Sea Research*, **33**, 1617–1640.

LEGECKIS R. (1978) A survey of worldwide sea surface temperature fronts detected by environmental satellites. *Journal of Geophysical Research*, **83**, 4501–4522.

LEGECKIS R. and A. L. GORDON (1982) Satellite observations of the Brazil and Falkland Currents—1975 to 1976 and 1978. *Deep-Sea Research*, **29**, 375–401.

LUSQUIÑOS A. and A. J. VALDEZ (1971) Aportes al conocimiento de las masas de agua del Atlántico sudoccidental *Publceción Servicio* de *Hidrografia Naval H659*, Buenos Aires, Argentina, 48 pp.

MCCLAIN E. P., W. G. PICHEL, C. C. WALTON, Z. AHMED and J. SUTTON (1983) Multi-channel improvements to satellite derived global sea surface temperatures. *Proceedings of XXIV COSPAR, Advances in Space Research*, **2**, 43–47.

MCCLAIN E. P., W. G. PICHEL and C. C. WALTON (1985) Comparative performance of AVHRR-based multichannel sea surface temperatures. *Journal of Geophysical Research*, **90**, 11,587–11,601.

MOORE D. W. and P. P. NIILER (1974) A two-layer model for the separation of inertial boundary currents. *Journal of Marine Research*, **32**, 457–484.

MORGAN G. W. (1956) On the wind-driven ocean circulation. *Tellus*, **8**, 301–320.

MULHEARN P. J. (1987) The Tasman Front: A study using satellite infra-red imagery. *Journal of Physical Oceanography*, **17**, 1148–1155.

MUNK W. H. (1950) On the wind-driven ocean circulation. *Journal of Meteorology*, **7**, 79–93.

NIILER P. P., R. E. DAVIS and H. J. WHITE (1987) Water-following characteristics of a mixed layer drifter. *Deep-Sea Research*, **34**, 1867–1882.

NILSSON C. S. and G. R. CRESSWELL (1980) The formation and evolution of East Australian Current warm-core eddies. *Progress in Oceanography*, **9**, 133–183.

OU H. W. and W. P. M. DE RUIJTER (1986) Separation of an inertial boundary current from a curved coastline. *Journal of Physical Oceanography*, **16**, 280–289.

PARSONS A. T. (1969) A two-layer model of Gulf Stream separation. *Journal of Fluid Mechanics*, **39**, 511–528.

PRABHAKARA C., G. DALU and V. G. KUNDE (1974) Estimation of Sea Surface Temperature from remote sensing in the 11 μm to 13 μm window region. *Journal of Geophysical Research*, **79**, 1744–1749.

REID J. L., W. D. NOWLIN, Jr and W. C. PATZERT (1977) On the characteristics and circulation of the Southwestern Atlantic Ocean. *Journal of Physical Oceanography*, **7**, 62–91.

RICHARDSON W. S., W. J. SCHMITZ and P. P. NIILER (1969) The velocity structure of the Florida Current from the Straits of Florida to Cape Fear. Frederick C. Fuglister Sixtieth Anniversary Volume. *Deep-Sea Research*, **16**, Suppl., 225–231.

ROBINSON A. R. (1965) Three-dimensional model of inertial currents in a variable-density ocean. *Journal of Fluid Mechanics*, **21**, 211–223.

RODEN G. I. (1986) Thermohaline fronts and baroclinic flow in the Argentine Basin during the austral Spring of 1984. *Journal of Geophysical Research*, **91**, 5075–5093.

RYZHKOV YU. G. (1966) Eddies with horizontal axes above the edge of the continental shelf of South America. *Izvestya, Atmospheric and Oceanic Physics*, **2**, 49–51.

SCHEMAINDA R. (1980) Ergebnisse ozeanologischer Untersuchungen mit dem FFS "Ernst Haeckel" im Konvergenzgebiet von Brasil- und Falklandsstrom im Juni/Juli 1978. *Beitrage zur Meereskunde*, **44/45**, 109–121.

SCHWALB A. (1978) The TIROSN/NOAA A–G satillite series. NOAA TM NESS *95*. U.S. Government Printing Office, Washington, D.C., 75 pp. Available from NTIS.

SMITH N. R. and C. B. FANDRY (1976) A simple topographic model of Gulf Stream separation. *Journal of Physical Oceanography*, **6**, 22–28.

SPEIGEL E. and A. R. ROBINSON (1968) Inertial boundary currents in a stratified ocean. *Journal of Fluid Mechanics*, **32**, 569–607.

STOMMEL H. (1948) The westward intensification of wind-driven ocean currents. *Transactions of the American Geophysical Union*, **29**, 202–206.

SZPIGANOWICZ B. (1983) Contents of oxygen and nutrients in the frontal zone of the Brazil and Falkland currents. *Oceanologia*, **XX**, 168–186.

TOMOSADA A. (1986) Generation and decay of Kuroshio warm-core rings. *Deep-Sea Research*, **33**, 1475–1486.

TSENG Y. C. (1974) Study of the surface boundary of the Brazil and Falkland Currents. *Proceedings of the Seminar on Space Applications of Direct Interest to Developing Countries*, Vol. 2, Sao Jose dos Campos, Brazil, pp. 160–173.

TSENG Y. C., H. M. INOSTROZA and R. KUMAR (1977) Study of the Brazil and Falkland Currents using THIR images of NIMBUS V and oceanographic data in 1972 to 1973. *Proceedings of the Eleventh International Symposium on Remote Sensing of Environment 25–29 April*, 1977, Vol. 1, Ann Arbor, U.S.A., pp. 859–871.

VERONIS G. (1973) Model of world ocean circulation. I. Wind-driven, two-layer. *Journal of Marine Research*, **31**, 228–288.

WARNECKE G., L. J. ALLISON, L. M. MCMILLIN and K. H. SZEKIELDA (1971) Remote sensing of ocean currents and sea surface temperature changes observed from the Nimbus II satellite. *Journal of Physical Oceanography*, **1**, 45–66.

WARREN B. A. (1963) Topographic influences on the path of the Gulf Stream. *Tellus*, **15**, 167–183.

WHITWORTH T. (1983) Monitoring the transport of the Antarctic Circumpolar Current at Drake Passage. *Journal of Physical Oceanography*, **13**, 2045–2057.

ZYRYANOV V. N. and D. N. SEVEROV (1979) Water circulation in the Falkland–Patagonia region and its seasonal variation. *Oceanology*, **19**, 518–522.